Materials Science and Engineering C 45 (2014) 210–215

Contents lists available at ScienceDirect

Materials Science and Engineering C

journal homepage: www.elsevier.com/locate/msec

Application of CdO nanoparticle ionic liquid modified carbon paste electrode as a high sensitive biosensor for square wave voltammetric determination of NADH

Ali Pahlavan [a,*], Hassan Karimi-Maleh [b,*], Fatemeh Karimi [c], Mohsen Aboukazempour Amiri [d], Zahra Khoshnama [e], Mandana Roodbari Shahmiri [f], Mohsen Keyvanfard [c]

[a] Department of Physics, Sari Branch, Islamic Azad University, Sari, Iran
[b] Department of Chemistry, Graduate University of Advanced Technology, Kerman, Iran
[c] Department of Chemistry, Majlesi Branch, Islamic Azad University, Isfahan, Iran
[d] Department of Biotechnology, Faculty of Chemical engineering, Mazandaran University of Science & Technology (MUST), Babol, Iran
[e] Department of Physics, Mazandaran Science and Research Branch, Mazandaran, Iran
[f] Department of Solid State Physics, University of Mazandaran, Babolsar, Iran

ARTICLE INFO

Article history:
Received 7 April 2014
Received in revised form 17 August 2014
Accepted 11 September 2014
Available online 16 September 2014

Keywords:
NADH
CdO nanoparticles
Ionic liquid
Electrochemical impedance spectroscopy
Voltammetry

ABSTRACT

In this paper we report the synthesis and application of CdO nanoparticle (CdO/NPs) and 1,3-dipropylimidazolium bromide as high sensitive sensors for voltammetric determination of nicotinamide adenine dinucleotide (NADH) using carbon paste electrode. The cyclic voltammogram showed an irreversible oxidation peak at 0.68 V (vs. $Ag/AgCl_{sat}$), which corresponded to the oxidation of NADH. Compared to common carbon paste electrode, the electrochemical response was greatly improved for NADH electrooxidation at a surface of CdO/NP modified ionic liquid carbon paste electrode (IL/CdO/NP/CPE). The linear response range and detection limit were found to be 0.09–750 μmol L^{-1} and 0.05 μmol L^{-1}, respectively. Result shows that other physiological species did not interfere in the determination of NADH at the surface of the proposed sensor in the optimum condition. The proposed sensor was successfully applied for the determination of NADH in tap water, urine and pharmaceutical serum samples.

1. Introduction

NADH is a coenzyme for more than 350 dehydrogenases, being involved in a wide range of enzymatic reactions. In living cells, it is involved in the production of adenosine triphosphate, compound that regulates the energy release from cells [1]. The NADH and its oxidized form, NAD^+, are ubiquitous bio-molecules found in both eukaryotic and prokaryotic organisms [2]. According to the above points, there is a great deal of interest in the development of new strategy for determination of NADH oxidation in biological systems. Due to its importance NADH as a cofactor for dehydrogenase enzymes and its role in the electron-transfer chain in biological system, electrochemical investigation of NADH has attracted considerable attention in the recent years. On the other hand, direct electrochemical detection by oxidation of NADH to its corresponding oxidized form NAD^+ at bare electrodes is accompanied by very high overpotential [3]. For this reason, the use of modified electrodes are necessary to obtain a suitable sensor with as high as possible a rate constant for NADH oxidation at the lowest possible overpotential, which are both important parameters for successful applications in biosensors and biofuel cells [4].

Nanoscience and nanotechnology represent new and enabling platforms that promise to provide a broad range of novel uses and improved technologies for environmental, biological and other scientific applications [5]. Materials in the nanoscale such as graphene, nanoparticles, carbon nanotubes and nanocomposite are being used for several analytical and bioanalytical applications [6–10]. Electrochemical analysis is taking advantages from all the possibilities offered by nanocompounds easy to be detected by conventional electrochemical methods [11–16].

Room temperature ionic liquid (RTIL) has been used as a new kind of modifier for a chemically modified electrode in the recent years [17–20]. The room temperature ionic liquids are composed entirely of ions and exist as a liquid at room temperature with the characteristics of negligible vapor pressure and good solubility and chemical stability [21–24]. As a novel green media, the RTIL has many unique optical and electrochemical properties, such as higher ionic conductivity and wider electrochemical windows [25–28].

In this work, we describe the synthesis and application of a novel CdO/NP modified ionic liquid carbon paste electrode, which utilizes 1,3-dipropylimidazolium bromide as a binder. The electrochemical behavior of NADH at IL/CdO/NP/CPE, at a surface of carbon paste electrode

* Corresponding authors.
E-mail addresses: pahlavan1292000@yahoo.com (A. Pahlavan), h.karimi.maleh@gmail.com (H. Karimi-Maleh).

http://dx.doi.org/10.1016/j.msec.2014.09.013
0928-4931/

modified with ionic liquid (IL/CPE), at CdO/NP carbon paste electrode (CdO/NP/CPE), and at carbon paste electrode (CPE) was investigated. The results showed the superiority of IL/CdO/NP/CPE to the other electrodes in terms of better reversibility and higher sensitivity. The proposed method is selective and sensitive enough for the determination of NADH in real samples.

2. Experimental

2.1. Chemicals

All chemicals used were of analytical reagent grade purchased from Merck (Darmstadt, Germany) unless otherwise stated. Doubly distilled water was used throughout. Phosphate buffer (sodium dihydrogen phosphate and disodium monohydrogen phosphate plus sodium hydroxide, 0.1 mol L^{-1}) solutions (PBS) with different pH values were used.

High viscosity paraffin ($d = 0.88$ kg L^{-1}) and pure graphite powder (particle size < 50 μm) from Merck was used for the preparation of the carbon paste electrodes.

2.2. Apparatus

Cyclic voltammetry, electrochemical impedance spectroscopy, and square wave voltammetry were performed in an analytical system, Autolab with PGSTAT 302N (Eco Chemie, the Netherlands). The system was run on a PC using GPES and FRA 4.9 software. For impedance measurements, a frequency range of 100 kHz to 0.1 Hz was employed. The AC voltage amplitude used was 5 mV, and the equilibrium time was 15 min. A conventional three-electrode cell assembly consisting of a platinum wire as an auxiliary electrode and an $Ag/AgCl/KCl_{sat}$ electrode as a reference electrode was used. The working electrode was either an IL/CdO/NP/CPE.

2.3. Synthesis of CdO/NPs

To prepare the CdO/NPs, in a typical experiment, a 0.5 M aqueous solution of $Cd(NO_3)_2$ and a 0.25 M aqueous solution of sodium hydroxide (NaOH) were prepared in distilled water. Then, the beaker containing NaOH solution was heated at the temperature of about 60 °C. The $Cd(NO_3)_2$ solutions were added drop wise (slowly for 2.0 h) to the above heated solution under high-speed stirring. The beaker was sealed at this condition for 2 h. The precipitated $Cd(OH)_2$ was cleaned with deionized water and ethanol then calcined at 400 °C for 2.0 h for synthesis of CdO/NPs.

2.4. Preparation of the modified electrode

IL/CdO/NP/CPE was prepared by mixing 0.1 g of 1,3-dipropylimidazolium bromide, 0.8 g of liquid paraffin, 0.2 g of CdO/NPs and 0.9 g of graphite powder. Then the mixture was mixed well for 50 min until a uniformly wetted paste was obtained (see Fig. 1). A portion of the paste was filled firmly into a glass tube as described above to prepare IL/CdO/NP/CPE. When necessary, a new surface was obtained by pushing an excess of the paste out of the tube and polishing it on a weighing paper.

2.5. Preparation of real samples

Urine samples were stored in a refrigerator immediately after collection. Ten milliliters of the sample was centrifuged for 35 min at 2000 rpm. The supernatant was filtered using a 0.45 mm filter and then diluted 5 times with the phosphate buffer, pH 7.0. The solution was transferred into the voltammetric cell to be analyzed without any further pretreatment. The standard addition method was used for NADH determination in real samples. Also, water and pharmaceutical serum samples were directly subjected to the voltammetric measurement of NADH.

Fig. 1. A typical picture of the modified electrode.

3. Results and discussion

3.1. CdO/NP characterization

The XRD patterns of the CdO nanoparticles showed diffraction peaks absorbed at 2θ values (Fig. 2). The prominent peaks have been utilized to estimate the grain size of sample with the help of Scherrer equation $D = K\lambda / (\beta\cos\theta)$ where K is a constant (0.9), λ is the wavelength (λ = 1.5418 Å), ß is the full width at the half-maximum of the line and θ is the diffraction angle. The grain size estimated using the relative intensity peak (111) for CdO nanoparticles was found to be 17.5 nm and increase in sharpness of XRD peaks indicates that particles are in

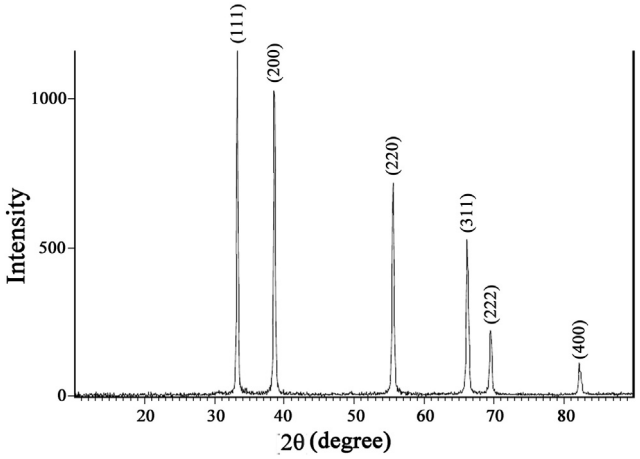

Fig. 2. XRD patterns of as-synthesized CdO/NPs.

crystalline nature. The (111), (200), (220), (311), (222) and (400) reflections are clearly seen and closely match the reference patterns for CdO (Joint Committee for Powder Diffraction Studies (JCPDS) File No. 05-0640) [29]. The morphology of the as-grown nanostructures was characterized by TEM technique. Fig. 3a shows the TEM images of the product synthesized. The dark spots correspond to CdO/NPs, which were only synthesized in our synthesis condition. NPs with near-spherical shapes were synthesized. It is clear that, in this case, CdO nanoparticles were successfully prepared. Fig. 3b displays a typical morphology of modified electrode characterized by SEM. As shown in Fig. 3(b), CdO/NPs on the surface of modified carbon paste electrode distributed well.

3.2. Electrochemical investigation

The active surface areas of the working electrodes are estimated according to the slope of the I_P versus $\nu^{1/2}$ plot for a known concentration of $K_4Fe(CN)_6$, based on the Randles–Sevcik equation:

$$I_p = 2.69 \times 10^5 n^{3/2} A D^{1/2} \nu^{1/2} C_O \quad (1)$$

where I_{pa} refers to the anodic peak current, n the electron transfer number, A the surface area of the electrode, D_R the diffusion coefficient, C_0 the concentration of $K_4Fe(CN)_6$ and ν is the scan rate. For 1.0 mmol L^{-1} $K_4Fe(CN)_6$ in 0.10 mol L^{-1} KCl electrolyte with $n = 1$ and $D_R = 7.6 \times 10^{-6}$ cm s^{-1} and from the slope of the I_{pa}–$\nu^{1/2}$ relation, the microscopic areas were calculated. They were 0.20, 0.14, 0.12 and 0.09 cm^2 for IL/CdO/NP/CPE, IL/CPE, CdO/NP/CPE and CPE, respectively. The results show that presence of CdO/NPs and ILs together causes the increase of the active surface in modification of electrode. According to scientific investigations, nanomaterials have high surface area and can increase current density and sensitivity in modified electrodes [30]. On the other hand, to summarize contrary to the electrodes modified by unsupported organic phase the electrochemical generation of charge in IL deposit may generate the transfer of its component across liquid|liquid interface. These points can increase active surface area for modified electrode [31].

Standard solutions of NADH (80 μmol L^{-1}) was used to find the optimum pH of supporting electrolyte which is best suited for determination of NADH employing IL/CdO/NP/CPE. The influence of the pH on the oxidation peak current of NADH was investigated employing PBS. It was observed that as pH of the medium was gradually increased, the potential kept on shifting towards less positive values, suggesting the involvement of proton in the reaction (Fig. 4 inset). Over the pH range 5.0–8.0, the peak potential (E_p) for NADH oxidation is a linear function of pH. From the plot of E_p vs. pH, slopes of -68.8 mV pH^{-1} was obtained for NADH (Fig. 4) in the working pH range. The E_{pa} of NADH has linear

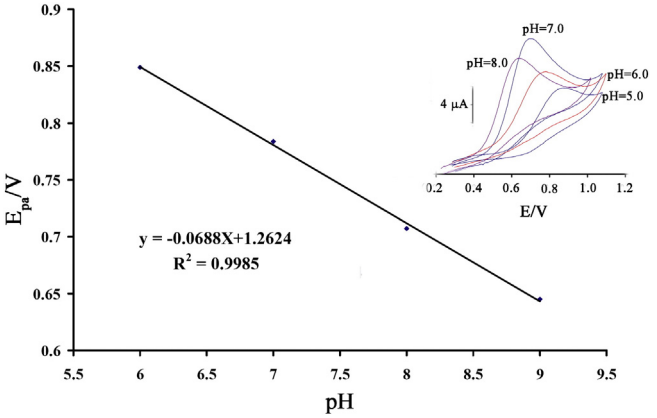

Fig. 4. Plot of potential, E, vs. pH for the electro-oxidation of 80 μmol L^{-1} NADH at a surface of IL/CdO/NPs/CPE. Inset: influence of pH on cyclic voltammograms of NADH at a surface of the modified electrode (pH 5–8, respectively).

relationship with pH of the buffer solution regarding the following equations:

$$E_p = -0.0688\ pH + 1.2624 \quad \left(R^2 = 0.9985\right). \quad (2)$$

This slope of -68.8 mV pH^{-1} reveal that an equal number of protons and electrons are involved in the oxidation reactions of NADH. It was observed that the peak current for NADH was maximum at pH 7.0 (not shown). Thus, this pH was employed for further studies. Various buffers, viz., phosphate, tris, citrate–phosphate and Britton–Robinson were then employed at pH 7.0. Out of these, pH 7.0 phosphate buffer solutions gave the best response in terms of peak current and peak shape and hence were employed as supporting electrolyte for further studies. In the next step, optimization of buffer concentration was carried out by varying its concentration in the range of 0.02–0.2 M. The best peak response was observed for 0.1 M of phosphate buffer and hence was used for further studies.

The cyclic voltammograms of NADH (50 μmol L^{-1}) at IL/CdO/NP/CPE, IL/CPE, CdO/NP/CPE and CPE are given in Fig. 5. It can be observed from the figure that moving from CPE to IL/CdO/NP/CPE, the anodic peak current of NADH increases and oxidation peak potential shifts to negative value simultaneously. It can also be observed that the background current is higher for IL/CdO/NP/CPE. This is due to the increased surface area of the electrode surface. Thus, the oxidation of NADH becomes facile on IL/CdO/NP/CPE.

The effect of potential scan rate on the peak current of NADH was also studied in the optimum condition. It can be seen that NADH (Fig. 6 inset)

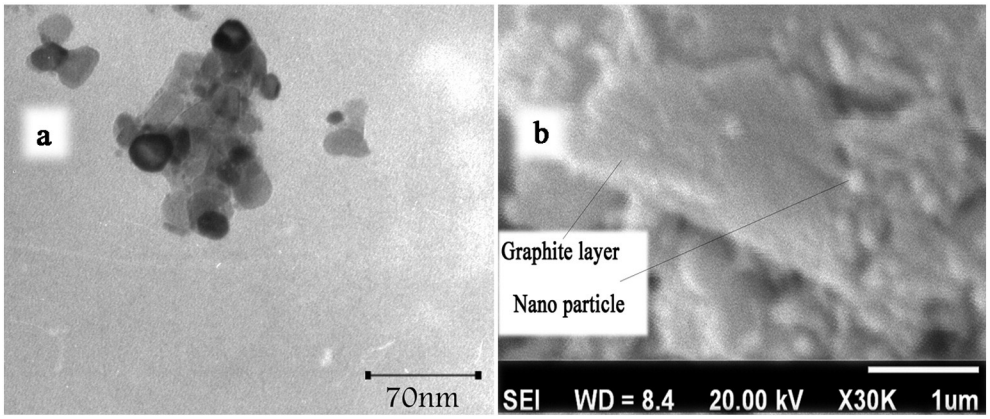

Fig. 3. a) TEM image of as-synthesized CdO/NPs. b) SEM images of modified electrode.

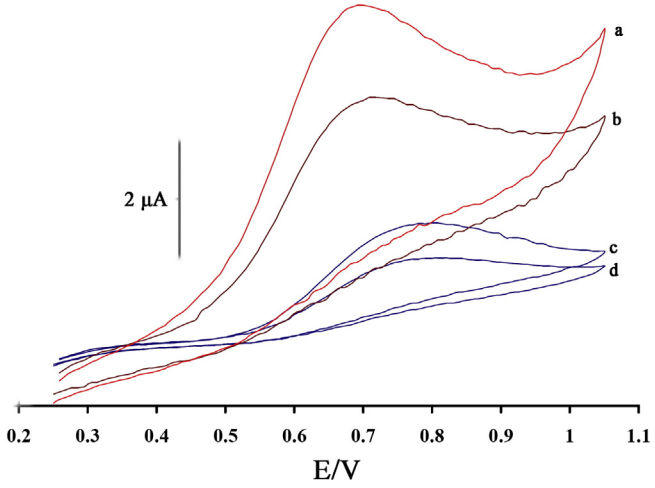

Fig. 5. Cyclic voltammograms of a) IL/CdO/NP/CPE, b) IL/CPE, c) CdO/NP/CPE and d) CPE in the presence of 50 μmol L^{-1} NADH at pH 7.0, respectively.

is completely irreversible in nature. From Fig. 6, it can be seen that the oxidation peak shifted to a more positive value for NADH with increasing scan rates along with a concurrent increase in current. The cyclic voltammetric results indicated that the anodic peak currents (i_p) of the molecule increase linearly with the square root of scan rate ($\nu^{1/2}$) in the range from 25 mV s^{-1} to 250 mV s^{-1} (Fig. 6). This finding implied that the oxidation of NADH is diffusion controlled on the IL/CdO/NP/CPE.

The dependence of the peak potential (E_{pa}) and ln(ν) showed a linear relationship with a regression equation of:

$$E_p = 0.0283\ \ln(\nu) + 0.7812\ \left(r^2 = 0.9935,\ E_p \text{ in V},\ \nu \text{ in V } s^{-1}\right). \quad (3)$$

According to the following equation [32]:

$$E_{pa} = E^{0/} + m\left[0.78 + \ln\left(D^{1/2}k_s^{-1}\right) - 0.5\ln m\right] + (m/2)\ \ln(\nu) \quad (4)$$

with

$$m = RT/[(1-\alpha)n_\alpha F. \quad (5)$$

The value of m = 0.0566 is calculated in Eq. (4). Therefore, the electron transfer coefficient (α) is approximately 0.55 for the irreversible electrode process.

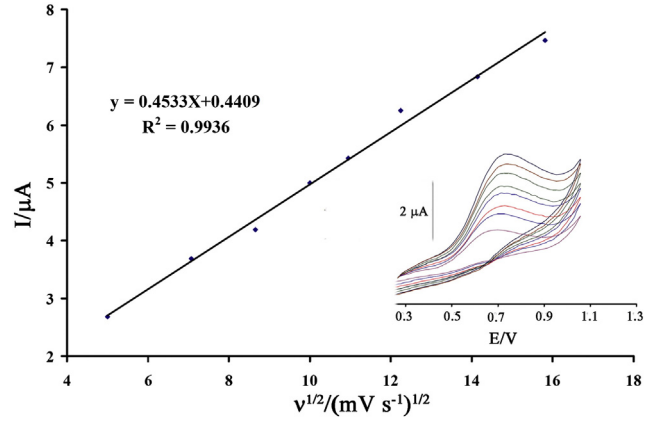

Fig. 6. Plot of I_{pa} versus $\nu^{1/2}$ for the oxidation of NADH at IL/CdO/NPs/CPE. Inset shows cyclic voltammograms of NADH at IL/CdO/NPs/CPE at different scan rates (from inner to outer) of 25, 50, 75, 100, 120, 150, 200 and 250 mV s^{-1} in 0.1 M phosphate buffer, pH 7.0.

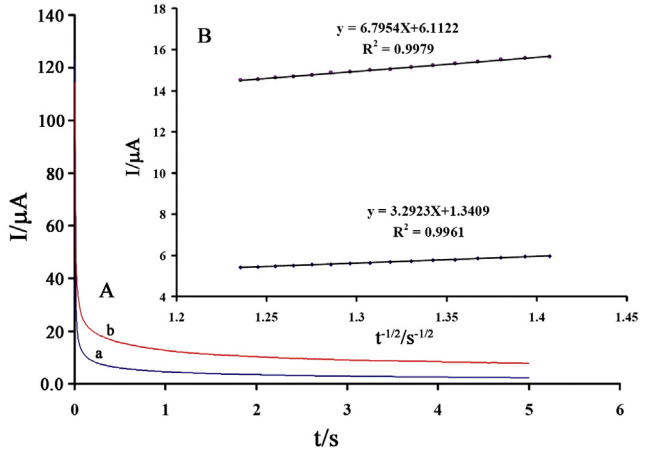

Fig. 7. A) Chronoamperograms obtained at IL/NiO/NP/CPE in the presence of a) 100; and b) 200 μmol L^{-1} NADH in the buffer solution (pH 7.0). B) Cottrell's plot for the data from the chronoamperograms.

The oxidation of NADH at the surface of IL/CdO/NP/CPE was also studied using chronoamperometry (Fig. 7A) method. Chronoamperometric measurements of different concentrations of NADH at the surface of the modified electrode were performed by setting the working electrode potential at 0.8 V vs. Ag/AgCl/KCl_{sat}. From the chronoamperometric study the diffusion coefficient, D, of NADH was determined in aqueous solution by using the Cottrell equation [33]:

$$I = nFACD^{1/2}\pi^{-1/2}t^{-1/2} \quad (6)$$

where C is the known concentration, D is the apparent diffusion coefficient, and A is the area of the electrode. The experimental plots of I vs. $t^{-1/2}$ for different concentrations of NADH were employed (Fig. 7B). The slopes of the resulting straight lines were then plotted vs. the NADH concentration. From the slope of the resulting plots and using the Cottrell equation, we calculated D as 9.2×10^{-6} cm^2 s^{-1}.

The electrochemical characterization of CPE, CdO/NP/CPE, IL/CPE and IL/CdO/NP/CPE was carried out by means of electrochemical impedance spectroscopy. The Nyquist plots for NADH (500 μmol L^{-1}) show a significant difference in the response for all the four electrodes as shown in Fig. 8. A semicircle with larger diameter is observed for CPE in the frequency range of 10^2–10^6 Hz. However, the diameter of semicircle diminished with the employment of IL/CdO/NP/CPE. This implies that charge transfer resistance of the electrode surface decreases and the charge transfer rate increases on employing IL/CdO/NP/CPE. The electrical

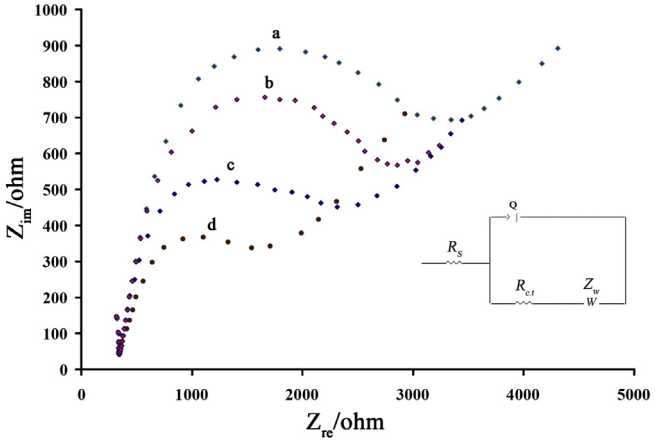

Fig. 8. Nyquist plots of CPE (a), CdO/NPs/CPE (b), IL/CPE (c), and IL/CdO/NPs/CPE (d) in the presence of 500 μmol L^{-1} NADH. Conditions: pH, 7.0; E_{dc}, +0.6 V vs. Ag/AgCl; E_{ac}, 5 mV; frequency range, 10^2–10^6 Hz. Inset: equivalent circuit for the system.

equivalent circuits (from the electrodes in the presence of NADH) compatible with the impedance spectra are shown in Fig. 8 inset. In this circuit, Rs, Q, and R_{ct} represent solution resistance, a constant phase element corresponding to the double-layer capacitance, and the charge transfer resistance associated with the oxidation of low valence mediator species. W is a finite-length Warburg short-circuit term coupled to R_{ct}.

3.3. Dynamic range and limit or detection

The calibration curve for NADH detection in pH 7.0 PBS was measured by SWV and two linear segments were observed. The initial linear portion increased from 0.09 to 30.0 μmol L^{-1} with a linear regression equation of i_{pa} (μA) = 0.2999 ± 0.0261 C (μmol L^{-1}) + 1.0967 ± 0.1621 (n = 6, R^2 = 0.9926). The second linear segment is from 30.0 up to 750.0 μmol L^{-1} with a linear regression equation of i_{pa} (μA) = 0.0607 ± 0.0024 C (μmol L^{-1}) + 7.9072 ± 0.5381 (n = 11, R^2 = 0.9944) (data obtained after base line correction). The difference in the slopes for the calibration curves is due to the different activities of the electrode surface with low and high concentration of the analyte. In the lower NADH concentration, due to a high number of active sites (in relation to the total number of the analyte molecules), the slope of the first calibration curve is high. While in the higher NADH concentration, due to decreasing active sites (in relation to the total number of analyte molecules, mainly at the surface of the electrode), sensitivity dramatically decreased and therefore, the second calibration slope decreased too. The detection limit of NADH was determined 0.05 μmol L^{-1} according to the definition of $Y_{LOD} = Y_B + 3\sigma$.

3.4. Interference studies

Interference studies were carried out with several chemical substances prior to the application of the proposed method for the assay of NADH in serum, water and urine samples. The potential interfering substances were chosen from the group of substances commonly found with NADH in pharmaceuticals and in biological fluids. The influence of various substances as potential interference compounds on the determination of 5.0 μmol L^{-1} NADH under the optimum conditions was studied. Tolerance limit was defined as the maximum concentration of the interfering substance that caused an error less than 3% in oxidation current of potential for the determination of NADH. After the experiments, we found that neither 1000-fold of glucose, sucrose, lactose, fructose, methanol and ethanol nor 700-fold of Br^-, K^+, Li^+, Cl^-, Ca^{2+}, Mg^{2+}, SO_4^{2-}, Al^{3+}, NH_4^+, F^-, Na^+ and ClO_4^-, nor 600-fold citric acid, methionine, alanine, phenylalanine, valine, tryptophan, glycine, valine, histidine and glutamic acid affected the selectivity. Nor did saturation of starch solution and 500-fold of urea, ascorbic acid (after addition 1 mM ascorbic oxidase) and thiourea were interfered with the determination of NADH. These results demonstrate that the modified electrode has a good selectivity for NADH analysis.

Table 1
Determination of NADH in real samples (n = 5).

Sample	Added (μmol L^{-1})	Expected (μmol L^{-1})	Founded (μmol L^{-1})	Recovery (%)
Urine	–	–	<Limit of detection	–
	1.0	1.0	1.05 ± 0.09	105.0
	10.0	10.0	10.72 ± 1.15	107.2
Tap water	–	–	<Limit of detection	–
	30.0	30.0	29.85 ± 0.72	99.5
	50.0	50.0	50.87 ± 1.22	101.7
Pharmaceutical serum	–	–	<LOD	–
	10.0	10.0	10.09 ± 0.35	100.9
	15.0	15.0	15.56 ± 0.75	103.7

± shows the standard deviation.

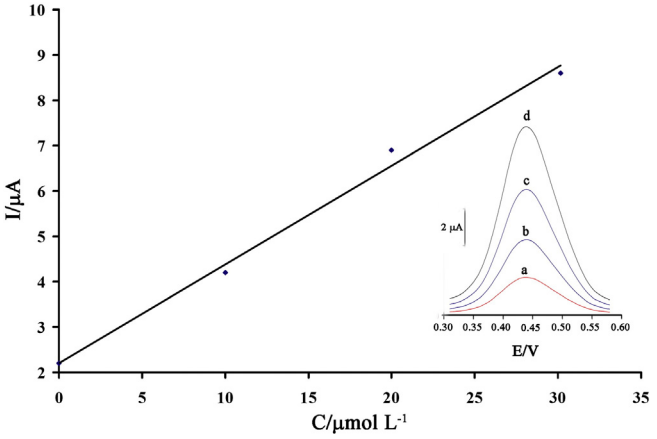

Fig. 9. Square wave voltammograms of IL/CdO/NPs/CPE in a solution containing 5.0 ml of the buffer (pH 7.0) and 5.0 ml of a serum sample for row no. 8 from Table 1. NADH added as a) 0.0, b) 10.0, c) 20.0, and d) 30.0 μmol L^{-1}.

3.5. Real sample analysis

In order to evaluate the analytical applicability of the proposed sensor, also it was applied to the determination of NADH in biological samples such as water, serum and urine. Standard addition method was used for measuring NADH concentration in the samples. A typical SWV for the determination of NADH in a urine sample (Table 1, row no. 8) is shown in Fig. 9. The results are given in Table 1; which confirm that the modified electrode retained its efficiency for the determination of NADH in real samples.

3.6. Stability and reproducibility of the modified electrode

The stability and reproducibility of any sensor are two important parameters for application of a suggestion sensor. Our experiments showed that after IL/CdO/NP/CPE was stored for 4 weeks at 4 °C, only a small decrease of peak current sensitivity with a relative standard deviation (RSD) of 1.7% (for 5.0 μmol L^{-1} NADH) was observed. This showed good stability of the modified electrode. Furthermore, the reproducibility of the determination was performed with seven successive scans in the solution containing 5.0 μmol L^{-1} NADH. The RSD values were found to be 2.1% for the analyte, indicating good reproducibility of the modified electrode. The electrode can be immersed in an aqueous media for 2.0 h with stable response. After that, the background current began to increase, which may be due to the partly leakage of ionic liquid from the electrode and the roughness of the electrode surface increases gradually.

4. Conclusion

The novel IL/CdO/NP/CPE was developed for the rapid determination of NADH in aqueous solution. IL/CdO/NP/CPE combines the features of CdO/NPs and room temperature ionic liquid to play a good voltammetric sensor for NADH analysis. Hence, it shows high sensitivity and reproducibility in sensing of NADH. Compared with traditional CPE, a decrease in overpotential of oxidation of NADH was about 120 mV with 4.0-fold increment in the oxidation peak current when using IL/CdO/NP/CPE as a sensor. Result confirms that the presence of CdO/NPs with high surface area and ILs with high conductivity structure can increase sensitivity proposed sensor for NADH analysis. The proposed method was successfully applied to the NADH detection in real samples.

Acknowledgments

The authors gratefully acknowledge the Graduate University of Advanced Technology, Kerman and Sari Branch, Islamic Azad University, Sari, for their support of this work.

References

[1] V. Lates, D. Gligor, L.M. Muresan, I.C. Popescu, Comparative investigation of NADH electrooxidation at graphite electrodes modified with two new phenothiazine derivatives, J. Electroanal. Chem. 661 (2011) 192–197.

[2] L. Zhang, Y. Li, L. Zhang, D.W. Li, D. Karpuzov, Y.T. Long, Electrocatalytic oxidation of NADH on graphene oxide and reduced graphene oxide modified screen-printed electrode, Int. J. Electrochem. Sci. 6 (2011) 819–829.

[3] C. Shan, H. Yang, D. Han, Q. Zhang, A. Ivaska, L. Niu, Electrochemical determination of NADH and ethanol based on ionic liquid-functionalized graphene, Biosens. Bioelectron. 25 (2010) 1504–1508.

[4] D. Gligor, Y. Dilgin, I.C. Popescu, L. Gorton, Poly-phenothiazine derivative-modified glassy carbon electrode for NADH electrocatalytic oxidation, Electrochim. Acta 54 (2009) 3124–3128.

[5] R. Sadeghi, H. Karimi-Maleh, A. Bahari, M. Taghavi, A novel biosensor based on ZnO nanoparticle/1,3-dipropylimidazolium bromide ionic liquid-modified carbon paste electrode for square-wave voltammetric determination of epinephrine, Phys. Chem. Liq. 51 (2013) 704–714.

[6] R. Moradi, S.A. Sebt, H. Karimi-Maleh, R. Sadeghi, F. Karimi, A. Bahari, H. Arabi, Synthesis and application of FePt/CNTs nanocomposite as a sensor and novel amide ligand as a mediator for simultaneous determination of glutathione, nicotinamide adenine dinucleotide and tryptophan, Phys. Chem. Chem. Phys. 15 (2013) 5888–5897.

[7] M. Roodbari Shahmiri, A. Bahari, H. Karimi-Maleh, R. Hosseinzadeh, N. Mirnia, Ethynylferrocene–NiO/MWCNT nanocomposite modified carbon paste electrode as a novel voltammetric sensor for simultaneous determination of glutathione and acetaminophen, Sensors Actuators B 177 (2013) 70–77.

[8] H. Karimi-Maleh, P. Biparva, M. Hatami, A novel modified carbon paste electrode based on NiO/CNTs nanocomposite and (9,10-dihydro-9,10-ethanoanthracene-11, 12-dicarboximido)-4-ethylbenzene-1,2-diol as a mediator for simultaneous determination of cysteamine, nicotine amide adenine dinucleotide and folic acid, Biosens. Bioelectron. 48 (2013) 270–275.

[9] B.J. Sanghavi, P.K. Kalambate, S.P. Karna, A.K. Srivastava, Voltammetric determination of sumatriptan based on a graphene/gold nanoparticles/Nafion composite modified glassy carbon electrode, Talanta 120 (2014) 1–9.

[10] B.J. Sanghavi, A.K. Srivastava, Adsorptive stripping differential pulse voltammetric determination of venlafaxine and desvenlafaxine employing Nafion–carbon nanotube composite glassy carbon electrode, Electrochim. Acta 56 (2011) 4188–4196.

[11] M.L. Yola, N. Atar, Z. Üstündağ, A.O. Solak, A novel voltammetric sensor based on p-amino thiophenol functionalized grapheme oxide/gold nanoparticles for determining quercetin in the presence of ascorbic acid, J. Electroanal. Chem. 698 (2013) 9–16.

[12] B.J. Sanghavi, S. Sitaula, M.H. Griep, S.P. Karna, M.F. Ali, N.S. Swami, Real-time electrochemical monitoring of adenosine triphosphate in the picomolar to micromolar range using graphene-modified electrodes, Anal. Chem. 85 (2013) 8158–8165.

[13] M.L. Yola, N. Atar, M.S. Qureshi, Z. Üstündağ, A.O. Solak, Electrochemically grafted todolac film on glassy carbon for Pb(II) determination, Sensors Actuators B 171–172 (2012) 1207–1215.

[14] M. Keyvanfard, R. Shakeri, H. Karimi-Maleh, K. Alizad, Highly selective and sensitive voltammetric sensor based on modified multiwall carbon nanotube paste electrode for simultaneous determination of ascorbic acid, acetaminophen and tryptophan, Mater. Sci. Eng. C 33 (2013) 811–816.

[15] A.A. Ensafi, H. Karimi-Maleh, S. Mallakpour, M. Hatami, Simultaneous determination of N-acetylcysteine and acetaminophen by voltammetric method using N-(3,4-dihydroxyphenethyl)-3,5-dinitrobenzamide modified multiwall carbon nanotubes paste electrode, Sensors Actuators B 155 (2011) 464–472.

[16] A.A. Ensafi, H. Karimi-Maleh, S. Mallakpour, B. Rezaei, Highly sensitive voltammetric sensor based on catechol-derivative-multiwall carbon nanotubes for the catalytic determination of captopril in patient human urine samples, Colloids Surf. B: Biointerfaces 87 (2011) 480–488.

[17] M. Najafi, M.A. Khalilzadeh, H. Karimi-Maleh, A new strategy for determination of bisphenol A in the presence of Sudan I using a ZnO/CNTs/ionic liquid paste electrode in food samples, Food Chem. 158 (2014) 125–131.

[18] A.L. Sanati, H. Karimi-Maleh, A. Badiei, P. Biparva, A.A. Ensafi, A voltammetric sensor based on NiO/CNTs ionic liquid carbon paste electrode for determination of morphine in the presence of diclofenac, Mater. Sci. Eng. C 35 (2014) 379–385.

[19] T. Jamali, H. Karimi-Maleh, M.A. Khalilzadeh, A novel nanosensor based on Pt:Co nanoalloy ionic liquid carbon paste electrode for voltammetric determination of vitamin B9 in food samples, LWT - Food Sci. Technol. 57 (2014) 679–685.

[20] A.A. Ensafi, H. Bahrami, B. Rezaei, H. Karimi-Maleh, Application of ionic liquid-TiO_2 nanoparticle modified carbon paste electrode for the voltammetric determination of benserazide in biological samples, Mater. Sci. Eng. C 33 (2013) 831–835.

[21] T. Tavana, M.A. Khalilzadeh, H. Karimi-Maleh, A.A. Ensafi, H. Beitollahi, D. Zareyee, Sensitive voltammetric determination of epinephrine in the presence of acetaminophen at a novel ionic liquid modified carbon nanotubes paste electrode, J. Mol. Liq. 168 (2012) 69–74.

[22] S. Salmanpour, T. Tavana, A. Pahlavan, M.A. Khalilzadeh, A.A. Ensafi, H. Karimi-Maleh, H. Beitollahi, E. Kowsari, D. Zareyee, Voltammetric determination of norepinephrine in the presence of acetaminophen using a novel ionic liquid/multiwall carbon nanotubes paste electrode, Mater. Sci. Eng. C 32 (2012) 1912–1918.

[23] H. Beitollah, M. Goodarzian, M.A. Khalilzadeh, H. Karimi-Maleh, M. Hassanzadeh, M. Tajbakhsh, Electrochemical behaviors and determination of carbidopa on carbon nanotubes ionic liquid paste electrode, J. Mol. Liq. 173 (2012) 137–143.

[24] E. Afsharmanesh, H. Karimi-Maleh, A. Pahlavan, J. Vahedi, Electrochemical behavior of morphine at ZnO/CNT nanocomposite room temperature ionic liquid modified carbon paste electrode and its determination in real samples, J. Mol. Liq. 181 (2013) 8–13.

[25] A. Taherkhani, T. Jamali, H. Hadadzadeh, H. Karimi-Maleh, H. Beitollahi, M. Taghavi, F. Karimi, ZnO nanoparticle-modified ionic liquid-carbon paste electrode for voltammetric determination of folic acid in food and pharmaceutical samples, Ionics 20 (2014) 421–429.

[26] J. Vahedi, H. Karimi-Maleh, M. Baghayeri, A.L. Sanati, M.A. Khalilzadeh, M. Bahrami, A fast and sensitive nanosensor based on MgO nanoparticle room-temperature ionic liquid carbon paste electrode for determination of methyldopa in pharmaceutical and patient human urine samples, Ionics 19 (2013) 1907–1914.

[27] M. Bijad, H. Karimi-Maleh, M.A. Khalilzadeh, Application of ZnO/CNTs nanocomposite ionic liquid paste electrode as a sensitive voltammetric sensor for determination of ascorbic acid in food samples, Food Anal. Methods 6 (2013) 1639–1647.

[28] M. Fouladgar, H. Karimi-Maleh, Ionic liquid/multiwall carbon nanotubes paste electrode for square wave voltammetric determination of methyldopa, Ionics 19 (2013) 1163–1170.

[29] S. Reddy, B.E. Kumara Swamy, U. Chandra, B.S. Sherigara, H. Jayadevappa, Synthesis of CdO nanoparticles and their modified carbon paste electrode for determination of dopamine and ascorbic acid by using cyclic voltammetry technique, Int. J. Electrochem. Sci. 5 (2010) 10–17.

[30] C.E. Banks, A. Crossley, C. Salter, S.J. Wilkins, R.G. Compton, Carbon nanotubes contain metal impurities which are responsible for the "electrocatalysis" seen at some nanotube-modified electrodes, Angew. Chem. Int. Ed. 45 (2006) 2533–2537.

[31] M. Mazloum-Ardakani, A. Khoshroo, High performance electrochemical sensor based on fullerene-functionalized carbon nanotubes/ionic liquid: determination of some catecholamines, Electrochem. Commun. 42 (2014) 9–12.

[32] R.S. Nicholson, I. Shain, Theory of stationary electrode polarography, Anal. Chem. 36 (1964) 706–723.

[33] A.J. Bard, L.R. Faulkner, Electrochemical Methods, second ed. Wiley, New York, 2001. 211.